Naval Research Laboratory

Washington, DC 20375-5320

Investigations of Polarization Dependent Loss in Polarization Modulated Analog Optical Links

Meredith N. Hutchinson
Nicholas J. Frigo

Photonics Technology Branch
Optical Sciences Division

Katrina E. Thompson

U.S. Naval Academy
Annapolis, Maryland

December 29, 2015

REPORT DOCUMENTATION PAGE

Public reporting burden for this collection of information is estimated to average 1 hour per response, including the time for reviewing instructions, searching existing data sources, gathering and maintaining the data needed, and completing and reviewing this collection of information. Send comments regarding this burden estimate or any other aspect of this collection of information, including suggestions for reducing this burden to Department of Defense, Washington Headquarters Services, Directorate for Information Operations and Reports (0704-0188), 1215 Jefferson Davis Highway, Suite 1204, Arlington, VA 22202-4302. Respondents should be aware that notwithstanding any other provision of law, no person shall be subject to any penalty for failing to comply with a collection of information if it does not display a currently valid OMB control number. **PLEASE DO NOT RETURN YOUR FORM TO THE ABOVE ADDRESS.**

1. REPORT DATE *(DD-MM-YYYY)* 29-12-2015	2. REPORT TYPE Memorandum	3. DATES COVERED *(From - To)* 21 July 2014 – 15 August 2014

4. TITLE AND SUBTITLE	5a. CONTRACT NUMBER
Investigations of Polarization Dependent Loss in Polarization Modulated Analog Optical Links	5b. GRANT NUMBER
	5c. PROGRAM ELEMENT NUMBER

6. AUTHOR(S)	5d. PROJECT NUMBER
Meredith N. Hutchinson, Nicholas J. Frigo, and Katrina E. Thompson*	5e. TASK NUMBER
	5f. WORK UNIT NUMBER 4973

7. PERFORMING ORGANIZATION NAME(S) AND ADDRESS(ES)	8. PERFORMING ORGANIZATION REPORT NUMBER
Naval Research Laboratory, Code 5651 4555 Overlook Avenue, SW Washington, DC 20375-5320	NRL/MR/5651--15-9658

9. SPONSORING / MONITORING AGENCY NAME(S) AND ADDRESS(ES)	10. SPONSOR / MONITOR'S ACRONYM(S)
Office of Naval Research One Liberty Center 875 North Randolph Street, Suite 1425 Arlington, VA 22203-1995	ONR
	11. SPONSOR / MONITOR'S REPORT NUMBER(S)

12. DISTRIBUTION / AVAILABILITY STATEMENT

Approved for public release; distribution is unlimited.

13. SUPPLEMENTARY NOTES

*U.S. Naval Academy, Physics Department M/S 9c, 572c Holloway Rd, Annapolis, MD 21402

14. ABSTRACT

This report describes a polarization modulated link and the associated polarization dependent loss, including theory. The general system is discussed as well as the details for measuring and calculating polarization dependent loss in the system. A set of experiments are presented that looks at non-ideal alignment of the polarization modulation arc. In addition to the theory for polarization distortion and a compensation technique, the system is investigated when only partially compensated for polarization dependent loss induced nonlinearity. Finally, the polarization modulator nonlinearities are investigated, with the results showing the tradeoffs for using either the DC bias of a rotating half-wave plate for bias phase control. The report also details the code that contains the model used to analyze the system.

15. SUBJECT TERMS

Fiber optics Polarization
Analog photonics

16. SECURITY CLASSIFICATION OF:			17. LIMITATION OF ABSTRACT	18. NUMBER OF PAGES	19a. NAME OF RESPONSIBLE PERSON Meredith N. Hutchinson
a. REPORT Unclassified Unlimited	b. ABSTRACT Unclassified Unlimited	c. THIS PAGE Unclassified Unlimited	Unclassified Unlimited	25	19b. TELEPHONE NUMBER *(include area code)* (202) 767-9549

TABLE OF CONTENTS

EXECUTIVE SUMMARY

A polarization modulated analog optical link is presented with theoretical treatment of nonlinearities due to polarization distortion loss (PDL). A method for measuring PDL within the system is detailed. A number of experiments are performed which characterize the modulator nonlinearity as well as the interaction of multiple nonlinearities. The primary findings include:

- Misalignment of the modulation arc induced second order nonlinearities and resembles the negatives effects imposed by chromatic dispersion.
- Partially compensating for PDL distortion resulted in non-conformal behavior for high RF power, indicating that multiple nonlinearities induce second order distortion.
- Polarization modulator nonlinearity contributes to second order distortion and indicated that suppression techniques cannot fully mitigate distortion at high RF power.

INVESTIGATIONS OF POLARIZATION DEPENDENT LOSS IN POLARIZATION MODULATED ANALOG OPTICAL LINKS

1 INTRODUCTION

High performance analog optical links for military applications primarily rely on the most common link architecture employing intensity modulation with direct detection (IMDD) due to the ease of implementation. Recently a special type of phase modulator employing TE and TM modulation, a polarization modulator (PolM), has gained interest in the field of microwave photonics. A PolM provides a constant intensity format that when aligned properly to a discriminator can function analogous to a Mach-Zehnder modulator (MZM) [1]. Many works have detailed the use of a PolM followed by a polarization controller (PC) which can be used to align to a polarization beam splitter (PBS) such that a photodetector can directly demodulate the signal [2-5], but have not detailed an algorithmic way in which to properly align the modulation arc and center the state of polarization (SOP) for maximum efficiency. In links employing polarization modulation, various processes can negatively impact performance such a polarization dependent loss (PDL), polarization mode dispersion (PMD), and chromatic dispersion (CD). For the purpose of this report we focus on the impact of PDL in such a system. Previously we have shown through first aligning a PolM for intensity demodulation followed by the addition of a known discrete source of PDL, the bias point of the link can be adjusted to cancel the second order distortion produced by PDL [6, 7].

This report will expand upon the work in [6] and [7], where first a general description of PDL in the system is discussed as well as the details by which we can measure and calculate the PDL through system diagnostics. Next a set of experiments are presented. First the system is analyzed for the ideal and a non-ideal alignment when no PDL is present. Next, the effect of including a discrete PDL and only partially compensating the resulting phase shift is presented. Additionally, when no PDL is present, we look at the difference in performance when adding a DC bias to the PolM and attempting to compensate the induced phase shift through rotating the half-wave plate at the discriminator. Finally we summarize the findings.

2 POLARIZATION DEPENDENT LOSS: THEORY AND SETUP

2.1 GENERAL THEORY OF PDL

The theoretical description relies on a simple model of PDL as an ideal partial polarizer, in Jones space [8]:

$$\mathbf{P} = \begin{bmatrix} 1 & 0 \\ 0 & t \end{bmatrix} = \left(\frac{1+t}{2} \right) \begin{bmatrix} 1 & 0 \\ 0 & 1 \end{bmatrix} + \left(\frac{1-t}{2} \right) \begin{bmatrix} 1 & 0 \\ 0 & -1 \end{bmatrix} \tag{1}$$

where we have expanded $\mathbf{P}$ in terms of the 2 × 2 identity matrix, σ_0, and the Pauli matrix σ_1. For Hermitian matrices, as expansion in the Pauli matrix basix set results in 4 numbers, of which three can be associated with the components of a 3-D vector, illustratively $\vec{P}$, in Stokes space [9] - [12]. In the simple particular case of (1), we can associate the operator

$$\mathbf{P} = \left(\frac{1+t}{2}\right)\sigma_0 + \left(\frac{1-t}{2}\right)\hat{e}_1 \cdot \left(\sigma_1 \hat{e}_1 + \sigma_2 \hat{e}_2 + \sigma_3 \hat{e}_3\right)$$

$$= p_0 \sigma_0 + \bar{P}\hat{P} \cdot \hat{\sigma} = p_0 \sigma_0 + \vec{P} \cdot \hat{\sigma}, \tag{2}$$

with average field transmission $p_0 = (1+t)/2$, pass eigenstate $\hat{P} = \hat{e}_1$, and PDL vector $\vec{P} = \bar{P}\hat{P}$, having differential field magnitude $\bar{P} = (1-t)/2$. We note for a general polarizer with $0 < t < 1$,

$$p_0^2 + \vec{P} \cdot \vec{P} = \frac{1+t^2}{2}$$

$$p_0^2 - \vec{P} \cdot \vec{P} = t \tag{3}$$

As shown earlier [11], [12], once the operator $\mathbf{P}$ is cast in form (2), it can be generalized to any eigenstate $\hat{P}$. Thus, the second line of (2) is general and describes any orientation for the pass state of the link PDL or the receiver's analyzer.

To motivate the impact of PDL impairments, we first examine the transformation of state $|s\rangle$ incident on a partial polarizer to its output state $|s_f\rangle$, in terms of the corresponding Stokes vectors $\vec{s}$ and $\vec{s}_f$. Since

$$\vec{s}_f = \langle s_f | \hat{\sigma} | s_f \rangle = \langle s | \mathbf{P}^\dagger \hat{\sigma} \mathbf{P} | s \rangle \tag{4}$$

And the norm of $\vec{s}$ is $|\vec{s}| = \langle s | s \rangle = s^2$, we find

$$\vec{s}_f = s^2 \left[\left(p_0^2 - P^2 \right) \hat{s} + 2 \left(p_0 + \vec{P} \cdot \hat{s} \right) \vec{P} \right], \tag{5}$$

Where $P^2 = \vec{P} \cdot \vec{P}$ and $\hat{s}$ is the unit Stokes vector for $\vec{s}$. From this, the power transmission is found as

$$T = \left(p_0^2 + P^2 \right) + 2 p_0 \left(\vec{P} \cdot \hat{s} \right), \tag{6}$$

Giving the expected transmission characteristic [16].

To illustrate the impact of PDL impairments, we examine the effect of $\mathbf{P}$ on states of polarization (SOPs) for several value of pass axis transmission, t. In Fig. 1, the outer spheres represent the unattenuated SOPs that could be incident on the partial polarizer. The partial polarizer is represented by an arbitrary $\vec{P}$: In this case, upward to the left, and "behind" the page. An arc of modulated SOPs is shown on the "far side" of the sphere, centered on the quiescent SOP, $\vec{s}_0$ at 90° to the $\hat{x}$ (or $\hat{e}_1$) vector in this Stokes/Poincare representation, as in Fig. 1(b). Such an arc of modulated SOPs would therefore be ideally biased. PDL, characterized by $\hat{P}$, distorts this ideal operation as indicated by the inner surfaces in each of the sub-figures, drawn to represent the transmitted power, T, for each SOP, as in (6). Four such surfaces, corresponding to different values of t in (1) are shown, with (a)-(d) running from 0.9 to 0.1. Also shown are the arcs, inside those surfaces, corresponding to SOPs emerging from the partial polarizer. For $t = 0.9$, Fig. 1(a), the input and output arcs are similar. For $t = 0.7$, Fig. 1(c), the presence

of a "dimple" in the rejected SOP (opposite to $\hat{P}$) is becoming evident [8], as well as indications that the arc is distorted in direction. For high PDL $t = 1$, Fig. 1(d), a dimple representing the rejected SOP's transmission is visible, and the transmitted SOPs are are nearly coincident with pass axis line.

We model the link as launch state $|s_0\rangle$ evolving under the operators for the modulator $(\mathbf{M})$, PDL $(\mathbf{P})$, and polarization discriminator $(\mathbf{D})$ operators. At the photodetector, output state $|s_f\rangle$ is given by

$$|s_f\rangle = \mathbf{D}\,\mathbf{P}\,\mathbf{M}\,|s_0\rangle \tag{7}$$

And the normalized optical intensity is found, through squaring its norm, as

$$i_{\text{det}} \approx \langle s_f | s_f \rangle = \langle s_0 | \mathbf{M}^\dagger \mathbf{P}^\dagger \mathbf{D}^\dagger \mathbf{D}\,\mathbf{P}\,\mathbf{M} | s_0 \rangle . \tag{8}$$

$\mathbf{P}$ and $\mathbf{D}$ are covered by (1)-(3), while $\mathbf{M}$ is modeled by

$$\begin{bmatrix} E_{x,out} \\ E_{y,out} \end{bmatrix} = \begin{bmatrix} e^{-j\phi/2} & 0 \\ 0 & e^{+j\phi/2} \end{bmatrix} \begin{bmatrix} E_{x,in} \\ E_{y,in} \end{bmatrix} = \mathbf{M}_0(\phi) \begin{bmatrix} E_{x,in} \\ E_{y,in} \end{bmatrix}, \tag{9}$$

Which introduces a phase difference of ϕ between the x and y components of the field. This can be expressed as

$$\mathbf{M}_0(\phi) = \begin{bmatrix} \cos(\phi/2) - j\sin(\phi/2) & 0 \\ 0 & \cos(\phi/2) + j\sin(\phi/2) \end{bmatrix},$$
$$= \cos(\phi/2)\sigma_0 - j\sin(\phi/2)\vec{M}\cdot\hat{\sigma} \tag{10}$$

where $\vec{M} = \hat{e}_1$ represents the slow eigenstate of the modulator. Again, a similarity transform allows this to be generalized to any $\vec{M}$ [11],[12].

Using form (3), and employing (10) for operator $\mathbf{M}$, we substitute (8) to solve for the photocurrent. Assuming a negligible dispersion and an ideal modulator, the detector photocurrent is given by

$$i_{\text{det}}(\phi) = \frac{1}{2}\left(c_1 + \vec{A}\cdot\vec{s}\right) + \left(\vec{A}\cdot\vec{M}\right)\left(\vec{M}\cdot\hat{s}\right) + \left[\vec{A}\times\vec{M}\cdot\hat{s} - \left(\vec{A}\cdot\vec{M}\right)\left(\vec{M}\cdot\hat{s}\right)\right]\sin\phi$$
$$+ \left[\frac{1}{2}\left(c_1 + \vec{A}\cdot\vec{s}\right) - \frac{\vec{M}\cdot\vec{M}}{2}\left(c_1 - \vec{A}\cdot\vec{s}\right)\right]\cos\phi \tag{11}$$

Where we have defined

$$\vec{A} = c_2\vec{P} + c_3\vec{D} \tag{12}$$

with

$$c_1 = \left(d_0^2 + \vec{D}\cdot\vec{D}\right)\left(p_0^2 + \vec{P}\cdot\vec{P}\right) + 4d_0 p_0 \vec{P}\cdot\vec{D}$$

3

$$c_2 = 2p_0\left(d_0^2 + \vec{D}\cdot\vec{D}\right) + 4d_0\vec{P}\cdot\vec{D}$$

$$c_3 = 2d_0\left(p_0^2 - \vec{P}\cdot\vec{P}\right) . \tag{13}$$

Eqn. (11) is the central theoretical result of our investigation. It is a description of the output photocurrent for a link with discrete PDL characterized by $\vec{P}$ (but otherwise ideal), expressed as a function of the applied modulator phase, ϕ, and the link parameters.

Before proceeding to the link analysis, we make contact with earlier work. For the special case of no modulator, $\phi = 0$ and $\vec{M} = 0$, and (11) reduces to

$$i_{\text{det}} = c_1 + \vec{A}\cdot\hat{s} . \tag{14}$$

This photocurrent is equivalent to the power transmission T and agrees with the general form in Ref. [13]. Furthermore, c_1 is an explicit form for the reference's Eqn. (5), and $\vec{A}$ is an explicit form for that reference's Eqn. (6). Thus, this special case of (11) agrees with the earlier transmission form and concatenation rule [13].

Returning to the link equations, (11), what is perhaps most surprising is that it has the general form

$$i_{\text{det}} = C_1 + C_2 \sin\phi + C_3 \cos\phi \tag{15}$$

With the constants C_i are defined explicitly in the equation. The last two terms are somewhat surprising. They imply that the time-varying signal, the part dependent on the modulator phase ϕ, is quite similar to the ideal behavior in a polarization modulated link. That is, the output in (11) is a sinusoidal variation in ϕ with amplitude $\sqrt{C_2^2 + C_3^2}$ and a phase offset of $\tan^{-1}\left(C_3/C_2\right)$. In other words, apart from the loss of signal, after accounting for all the distortions due to unintentional amplitude modulation and to arc re-orientation in Fig. 1, the output has exactly the same form as an ideal interferometer which happens to be biased off quadrature by $\tan^{-1}\left(C_3/C_2\right)$. To put this in context of Fig. 1, the projection onto the $\hat{x}$ for SOPs along each of the four arcs (i.e., using great circle arcs connecting each point to $\hat{x}$) is the same as the projection of the SOPs along the initial arc, after a slight displacement along the equator and an overall attenuation. We will experimentally demonstrate this counter-intuitive result.

Since $\vec{M}\cdot\vec{M} = 1$ for our assumed ideal modulator, we can simplify (11):

$$i_{\text{det}} = c_1 + \left(\vec{A}\cdot\vec{M}\right)\left(\vec{M}\cdot\vec{s}\right) + \left[\vec{A}\times\vec{M}\cdot\vec{s} - \left(\vec{A}\cdot\vec{M}\right)\left(\vec{M}\cdot\vec{s}\right)\right]\sin\phi + \vec{A}\cdot\vec{s}\cos\phi . \tag{16}$$

Further assuming a perfect polarizer at the receiver, it can be shown that (13) reduces to

$$c_1 = \frac{1+t^2}{4} + \frac{1-t^2}{4}\vec{P}\cdot\vec{D} = \frac{1}{2}\left[\cos^2\frac{\Phi}{2} + t^2\sin^2\frac{\Phi}{2}\right]$$

$$c_2 = \frac{1+t}{2} + \frac{1-t}{2}\vec{P}\cdot\vec{D} = \left[\cos^2\frac{\Phi}{2} + t\sin^2\frac{\Phi}{2}\right]$$

$$c_3 = t \tag{17}$$

4

Which leads to a direct expression for (12):

$$\vec{A} = \left[\cos^2 \frac{\Phi}{2} + t \sin^2 \frac{\Phi}{2} \right] \left(\frac{1-t}{2} \right) \hat{P} + \frac{t}{2} \hat{D}, \qquad (18)$$

Where Φ is the angle measure of the great circle arc that connects $\hat{P}$ to $\hat{D}$. For the ideal link, $t = 1$.
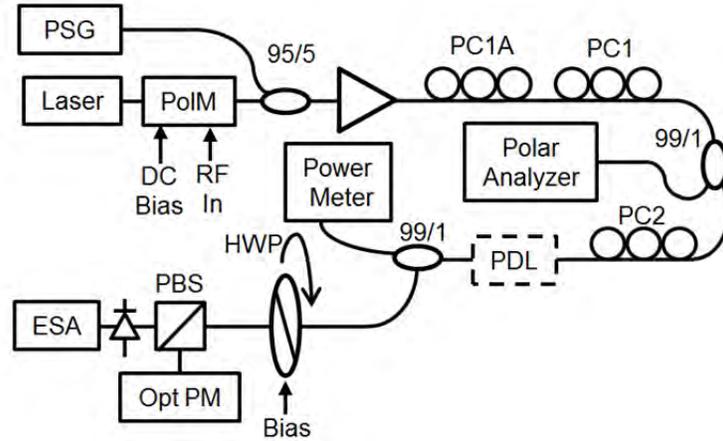
2.2 POLARIZATION MODULATION LINK SETUP

Fig. 2.1: Experimental Setup. Laser is polarization modulated (PolM), andlaunched into a short optical link. In ideal link, the modulated signal is developed with polarization beam splitter (PBS), detected with photodiode (PD), and the RF harmonics are analyzed with electrical spectrum analyzer (ESA). Polarization-dependent loss is introduced in a test jig (PDL). The relationship between the SOPs of the signal, the PBS, and the PDL are analyzed by introducing well-defined polarization states with a polarization state generator (PSG) and analyzed with reference to a polarimeter (Polar Analyzer). Rejected optical power is monitored (Opt PM) for diagnostics.

We constructed a basic link using a Versawave 40 Gb/s polarization modulator [14] that permitted both RF modulation and DC bias control. The light from a DFB laser, after modulation, passed through a coupler, was amplified, passed through a set of polarization controllers (PC1A, PC1) to a tap coupler. (We use two polarization controllers for experimental convenience: in effect we must set not only ~s0 on the correct point of the equator, but must also put the entire modulated arc on the equator [15].) At that tap coupler, a portion of the light was sent to a polarimeter (Polar Analyzer) which we used to monitor the experiment, as detailed below. Light from the other port was sent through another polarization controller (PC2) and then into a bulk beam expander and refocused back to fiber. The collimated beam in this beam expander was used to introduce the various PDL elements, as described below. For convenience, a half-wave plate (HWP) on a rotatable stage was mounted in a second bulk optic beam expander. This provided a reproducible way to apply and invert a set of polarization transformations, also described below. In ideal operation, the net result of the polarization evolution from the PolM output, through the link and HWP, to a polarization analyzer (bulk polarization beam splitting cube (PBS)), was that the light at the PBS input was polarized at quadrature, and the detected light at the photodetector (PD) mimicked an ideal interferometric link [16]. For diagnostic purposes, the power at the rejected PBS port and the DC photocurrent on the output photodiode were recorded. An electrical spectrum analyzer (ESA) was used to monitor the first 4 harmonics of the detected power spectrum as a means of quantifying PDL impairments introduced into the link.

To set up the idealized link, we followed a procedure established earlier [15] that ensures ideal operation by reproducibly orienting the modulated SOPs which enter the PBS. The link is then biased at quadrature, there is no PDL in the test jig, and the SOPs corresponding to the modulator eigenstate ~M and the PBS pass axis, ~D have images which are marked on the polarimeter in Fig. 2.3.

2.3 PDL MEASUREMENT ROUTINE

Once the operation of the link had been established, we then introduced PDL by dropping in a home-made test jig which held two uncoated optical flats held at various fixed angles. An angle-dependent PDL is introduced by tilting since the s- and p-polarized components striking both surfaces of a flat experience different Fresnel reflection coefficients [8]. We used two identical flats oriented with opposite angles, similar to an earlier description [17], so that the PDL is doubled while walkoff through the beam expander is cancelled. To measure the added PDL, the main laser is shut off. A polarization state generator (PSG) from General Photonics is used to generate a test signal that can scan through the 6 degenerate states. At each generated state the SOP at the PA is recorded as well as the optical power received at the power meter at the 1% tap of the coupler placed before the HWP. The measurement routine allows for the determination of the pass axis represented at the PA as well as the total PDL measured in the link through a Mathematica routine employing a least squares fit (Appendix A). The measured PDL can then be compared against the expected PDL determined by the theoretical calculations based on the angle of rotation of the optical flats. Ideally a system with no PDL will record constant optical power when performing a sweep with the PSG. As illustrated in Fig. 2.3, a shaded surface is shown inside the Poincare sphere which represents a discrete amount of PDL, where a dimple can be seen that is orthogonal to the pass axis. Thus one can conceptualize how the measurement of 6 points on the shaded surface can be translated into the approximate value of the total PDL as well as delineate the pass axis, all from the simple routine. Conceivably a well-designed system could incorporate a built-in PDL measurement function to measure the total PDL. It should be noted that this routine has only been used for one discrete source of PDL, when in fact the total system may contain more than one source of PDL. The theoretical development to handle such a scenario is ongoing.
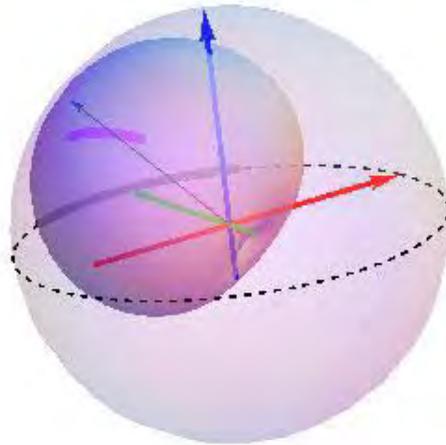

Fig. 2.3: Shaded surface graphs 60° PDL with a pass axis misaligned with the modulator pass axis. Orthogonal to the pass axis a dimple is observed in the PDL surface. The surface represents the non-uniform optical power loss at all SOPs. The black arc represents the ideal modulation arc along the great surface when no PDL is present. The altered modulation arc is shown in magenta where the arc is inside the Poincare sphere and shifted from the black arc.

Once a given PDL was introduced and the diagnostic routine described above was performed, we took a series of "characterization curves" to quantify the effect of the impairment. The characterization curves for each of the PDL levels were taken by applying sinusoidal 2 GHz signals (at a sequence of RF powers) to the polarization modulator's input port. Each RF power corresponds to a well-defined voltage excursion amplitude, which in turn corresponds to a well-defined arc length of SOPs. For each such input RF power level, we recorded and plotted the first four harmonic RF powers from the ESA. Even for ideal operation, one expects the transfer function (1) to generate odd harmonics of the 2 GHz fundamental, while that quadrature bias suppresses all even harmonics. We found that to fully characterize the outputs, all 4 harmonics were needed. In a separate experiment, the frequency-dependent RF losses of our coax cables were measured at all 4 harmonics to correct the raw data from the ESA. The details of measurements for PDL with optical flats at various angles the corresponding theoretical curves can be found in [6]. As detailed in the theoretical treatment of PDL in [6], PDL corresponds to a phase shift in the link which manifests as even-order distortion. Consequently, we detailed a procedure for mitigating the incurred even-order distortion through an appropriately applied DC bias voltage at the PolM or equivalently by rotating the HWP [7]. The primary focus of this report is to detail a series of experiments performed where we interrogated various performance aspects of the link in Fig. 2.1.

3 MISALIGNING THE MODULATION ARC

Up to this point the system has been operated by first performing the alignment procedure, where the center of modulation is located at 45 degrees to the pass axis and the modulation arc resides along the great circle as shown in solid red in Fig. 3.1. Previous work has described the effects of chromatic dispersion on a polarization modulated link, where the nonlinearity manifests as a misalignment in the arc [18]. We can simulate a similar case experimentally by purposefully misaligning the arc during our procedure, represented as shown in the dotted curve in Fig. 3.1. As with the polarization alignment procedure detailed previously, the SOP is aligned to the top of the sphere and represents the middle of the modulation arc (seen in Fig. 3.1 as the black dot) [1]. The arc must then pass through what is referred to as point B which will lie somewhere on the great circle when using the PA as the visualizer. The calibration procedure is first performed with proper alignment as described. The resulting fundamental and 2nd through 4th harmonics for a 2 GHz input signal as a function of input RF power are shown in black in Fig. 3.2. Next the alignment is adjusted such that a new B is recorded, designated B', which is misaligned by 10°. Again the fundamental, 2nd and 4th harmonics are recorded and plotted in Fig. 3.2 in blue, red and green respectively. Although the fundamental and 4th harmonic remain the same, the 2nd harmonic increases significantly at low input RF power. As has been shown previously, chromatic dispersion in an intensity modulated link results in increased second order distortion [19]. One could infer from this experiment that a well-controlled rotation of the modulation arc about the axis would allow one to probe the effects of chromatic dispersion in polarization modulated links more thoroughly with a combination of misaligned arc measurements and appropriate lengths of fiber to validate the results.
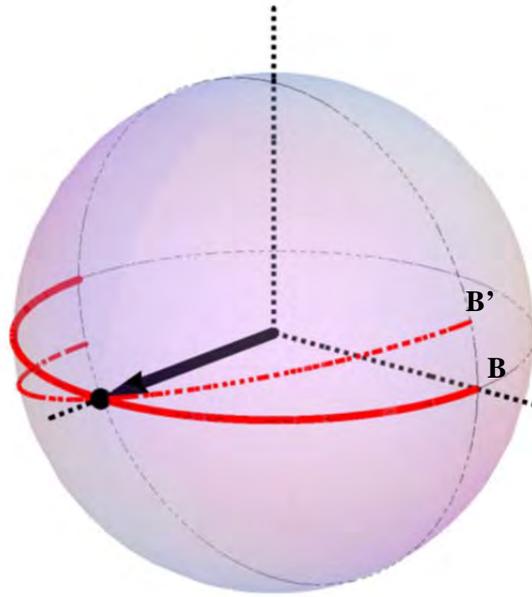
Fig. 3.1: Solid red arc shows ideal alignment at input to PBS. Arc is purposefully misaligned (red dotted) to investigate resulting nonlinearities.
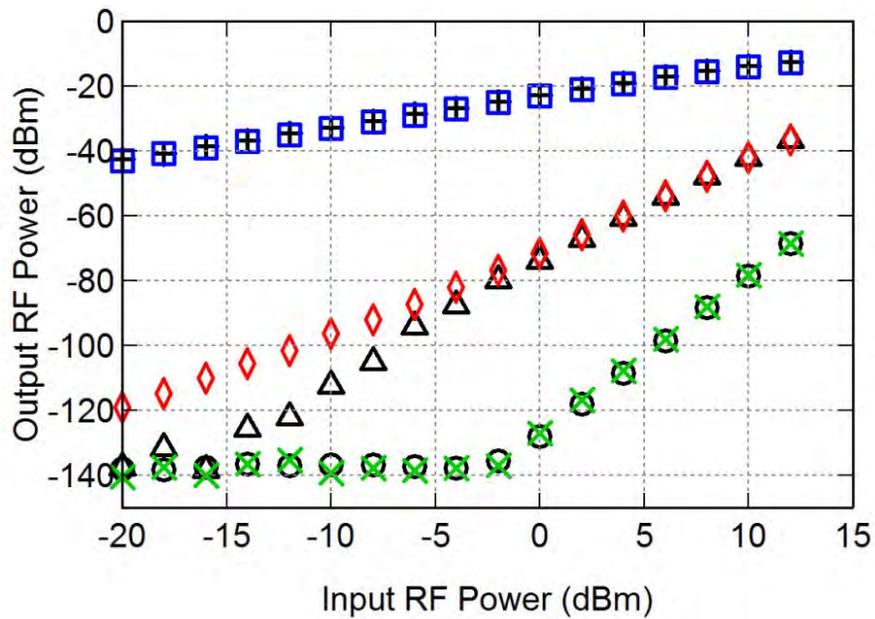

Fig. 3.2: Fundamental, 2nd and 4th harmonics for 2 GHz input signal for ideal aligned case (black) and with arc misaligned by 10° (color).

4 PARTIALLY COMPENSATING PDL WITH DC BIAS

As was theoretically and experimentally proven, PDL generated even-order distortion can be mitigated by properly adjusting the bias phase through either the DC bias or HWP [7]. In the next set of experiments we look at the effects on distortion for when the bias phase is not adjusted to the proper cancellation condition. In all the figures, the ideal data is shown in black, where the bias voltage was 4.1 V for a PDL of ~ 3dB. The colored data in Fig. 4.1 shows the PDL induced even order distortion, previously documented with the theory described in section 2, evident when no DC bias is applied and the HWP is left unaltered [6]. Using this as the reference point, in theory the curves should be between the red and black points for the 2nd harmonic shown in Fig. 4.1 and the green and black points for the 4th harmonic. In Fig. 4.2, 3 V is applied to the DC bias port, and as expected both the red and green data move closer to the ideal black data. Finally, the PDL is over compensated by applying 5 V (0.9 V more than the ideal condition of 4.1V). The red and green curves for low RF power do indeed behave as expected, where they are higher than the ideal data in black. However at higher RF power ($> 4dBm$) the red and green data are below the black data. When considering only one source of nonlinearity, the second order distortion will behave as a slope of two. However when the model incorporates multiple nonlinearities that may all have different phases, such as due to the PolM, the photodiode and polarization dependent loss, the second order distortion at the output becomes much more complicated. The model we have built in Mathematica (Appendix B), allows us to get a better picture of the different distortions that all interact within the system. However in order to tease out each nonlinearity a set of experiments needs to be determined to separate nonlinearities that are all on the same order of magnitude. If one nonlinearity is dominant, the model can easily predict the curves as was the case in our previous work [6]. The additional experiments to more thoroughly investigate the model are outside the scope of this report and will be left for future research.
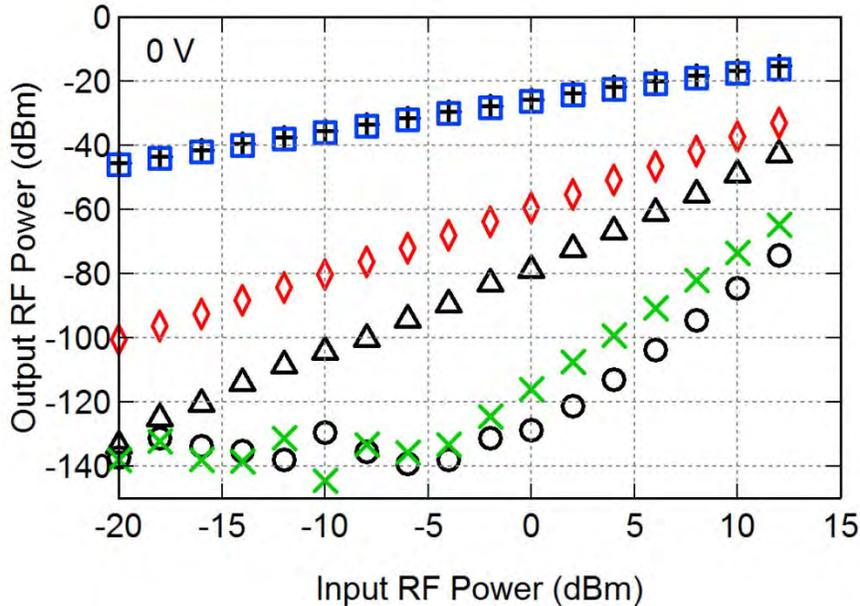

Fig. 4.1: PDL of ~ 3 dB (optical flats at 60 degree) is added to the system. Fundamental, 2nd and 4th harmonics are plotted for 2 GHz input. System is aligned and HWP is rotated to minimize 2nd order harmonic at -16 dBm input RF power, after which the PDL is added (Color). Same procedure as for data shown in color, but an additional 4.1 V bias is applied to the DC input of the PolM to minimize the 2nd harmonic at -16 dBm input RF power after adding PDL (Black).
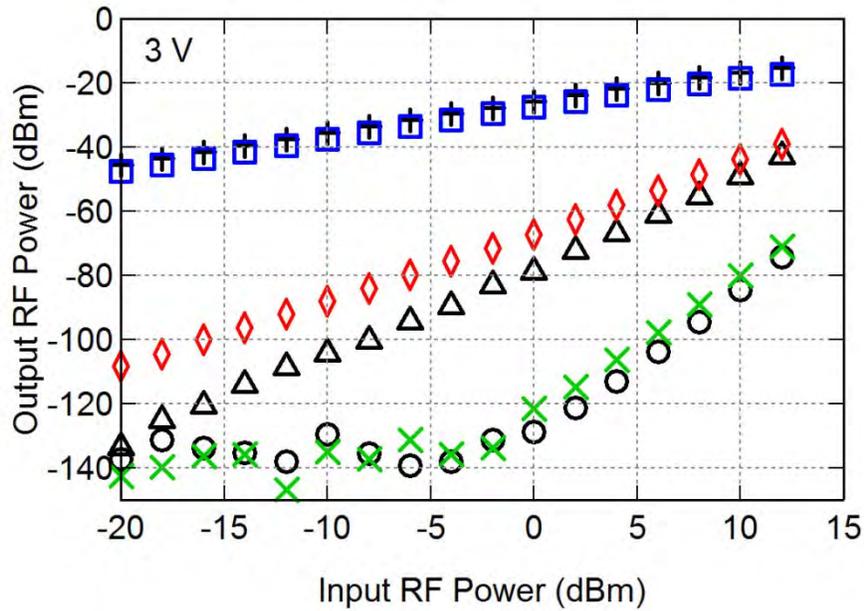
Fig. 4.2: Curves for 4.1 V bias applied after PDL added as seen in Fib 6a (Black). Experiment is repeated but only 3V of bias is applied to partially compensate 2nd harmonic distortion due to PDL (Color).
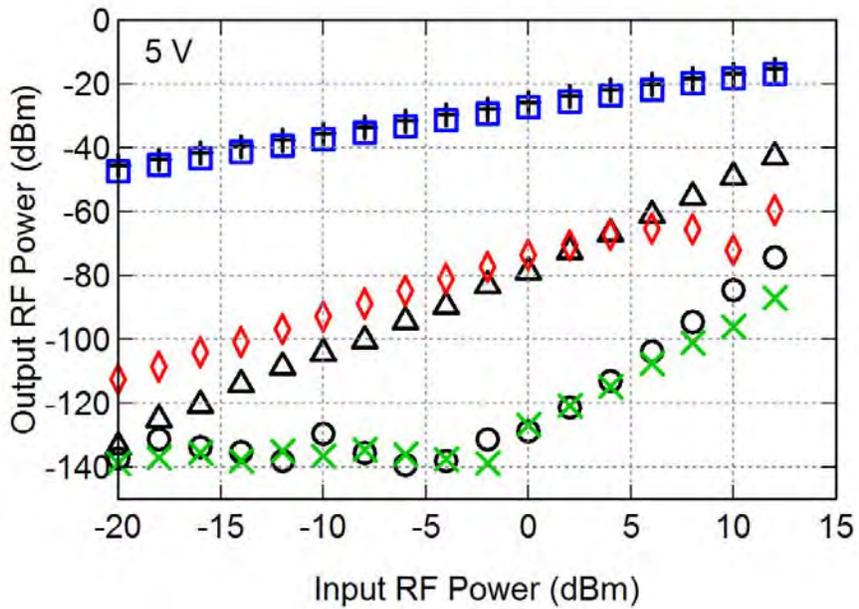

Fig. 4.3: Curves for 4.1 V bias applied after PDL added as seen in Fib 6a (Black). Experiment is repeated with 5 V bias applied to over compensate 2nd harmonic distortion due to PDL (Color).

5 INVESTIGATING NONLINEARITY IN A POLARIZATION MODULATOR

Lastly, a set of experiments were conducted to investigate the nonlinearity due to the PolM. It has been assumed up to this point that the DC bias at the PolM and the rotating HWP are equivalent in terms of bias phase control points. As was shown previously, the DC bias exhibits its own nonlinear optical transfer function that may impose such nonlinearity on the system. The link was setup and aligned as before initially with no DC bias applied. No PDL is added and the 2nd harmonic distortion is mitigated by adjusting the HWP properly. In the following figures, the resulting data from the fundamental, 2nd and 4th harmonics is plotted in black. Next we applied varying DC bias voltages to the PolM, followed by the alignment procedure. Finally the HWP is again rotated in order to mitigate the 2nd harmonic distortion. If adding a DC bias is equivalent to adjusting the HWP, the output of both experiments should be the same. Bias voltages of 3, 6, 8 and 10 V were tested with the output shown in Figs. 5.1-5.4 respectively. In the first case 3 V, the 4th harmonic is slightly reduced throughout, while the 2nd harmonic is the same at low and high RF power, but lower in the mid RF power range. Thus the distortion curves, particularly for the 2nd order distortion cannot be easily described by a slope of 2, as is generally thought of for 2nd order distortion. Clearly other nonlinearities that occur within the system dominate and potentially more than one, as the photodiode distortion is mostly mitigated. We find for the 6 V case that the curve shows more distortion at the low RF power and less at high RF power for the 2nd harmonic, so there isn't a clear benefit to using either the HWP or the DC bias. In the final two cases for 8 V and 10 V the 2nd harmonic again is similar at lower RF power, but significantly lower at high RF power, upwards of 15 dB near the 2 dB RF input point. The result of these measurements allows us to conclude that the distortion generated in the link does not behave as ideally as our model would suggest, and that the bias points can be potentially used in tandem to mitigate nonlinearity even further.
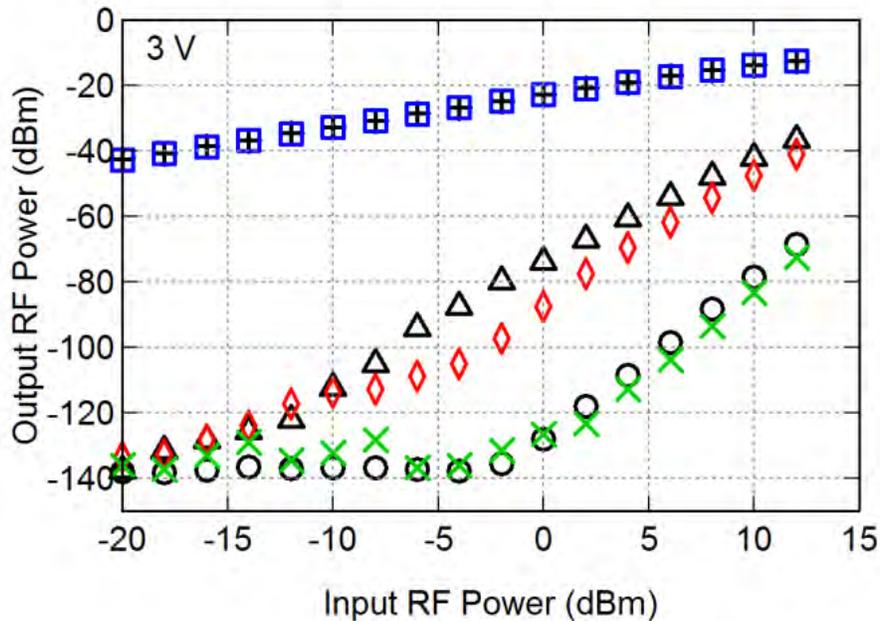

Fig. 5.1: Fundamental, 2nd and 4th harmonics are plotted for 2 GHz input. System is aligned and HWP is rotated to minimize 2nd order harmonic at -16 dBm input RF power (Black). Same procedure as for data shown in black except before alignment is performed a DC bias of 3V is added to the PolM (Color).
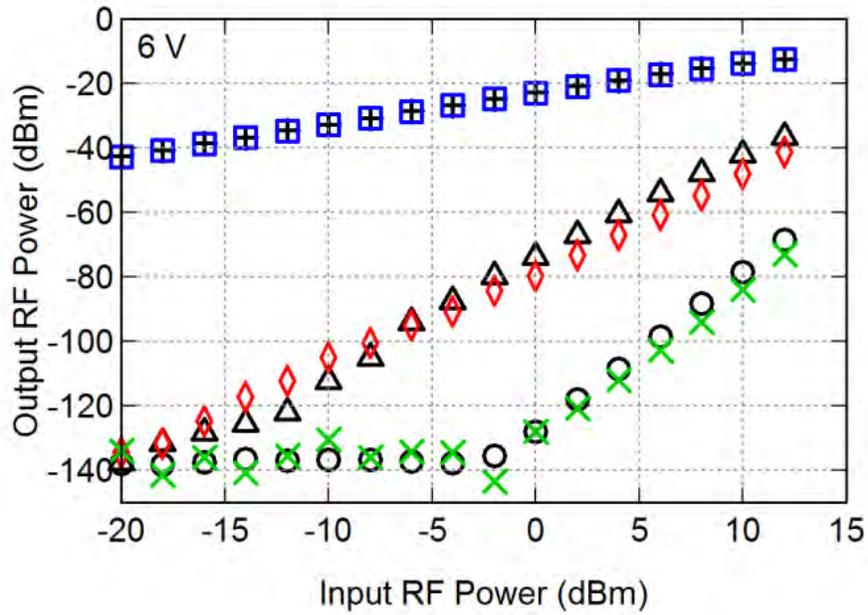
Fig. 5.2: Fundamental, 2nd and 4th harmonics are plotted for 2 GHz input. System is aligned and HWP is rotated to minimize 2nd order harmonic at -16 dBm input RF power (Black). Same procedure as for data shown in black except before alignment is performed a DC bias of 6 V is added to the PolM (Color).
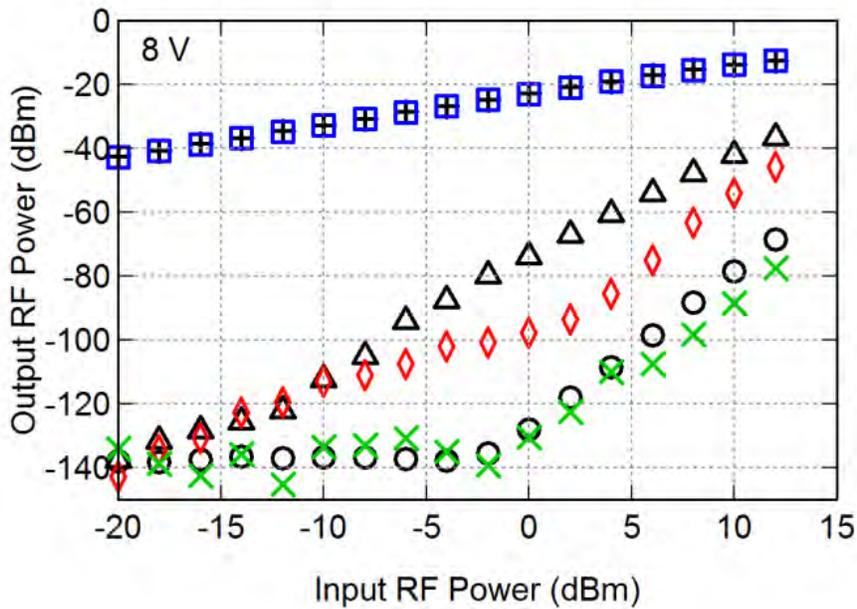

Fig. 5.3: Fundamental, 2nd and 4th harmonics are plotted for 2 GHz input. System is aligned and HWP is rotated to minimize 2nd order harmonic at -16 dBm input RF power (Black). Same procedure as for data shown in black except before alignment is performed a DC bias of 8 V is added to the PolM (Color).
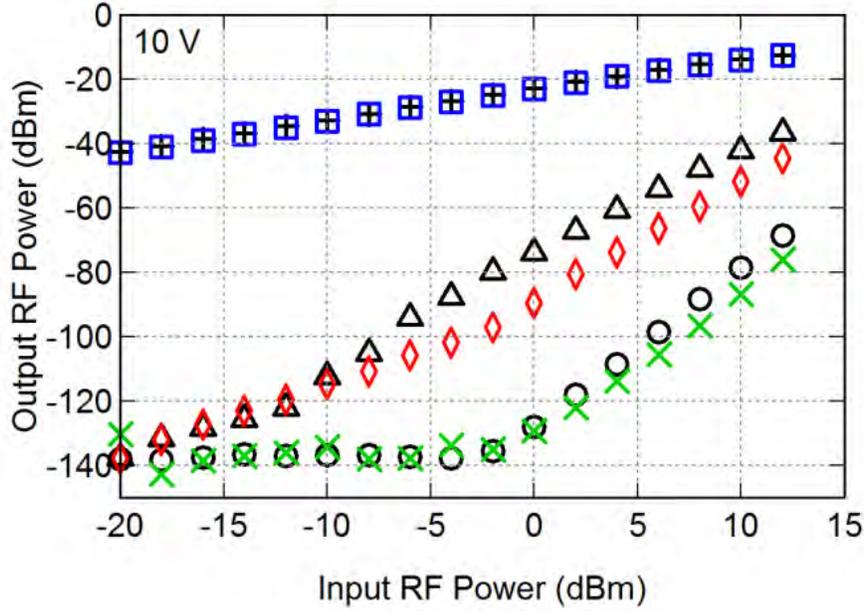
Fig. 5.4: Fundamental, 2nd and 4th harmonics are plotted for 2 GHz input. System is aligned and HWP is rotated to minimize 2nd order harmonic at -16 dBm input RF power (Black). Same procedure as for data shown in black except before alignment is performed a DC bias of 10V is added to the PolM (Color).

\

6 SUMMARY AND CONCLUSIONS

In summary the theory for a discrete PDL in a polarization modulated link was detailed. The link was presented along with the measurement routine needed to measure PDL in the system. The link alignment for optimal intensity modulation at the output is done before PDL is added to the system, which does not represent a real world case where unknown PDL would be part of the system before alignment. None the less the link was characterized for cases when the modulation arc is slightly misaligned, which shows contributed second order nonlinearity and the experiment is similar to the arc rotation that occurs with chromatic dispersion. A set of experiments were performed to investigate partially compensating the PDL. The results indicate that multiple nonlinearities are acting within the link and their additive magnitudes and phases provide a much more complex result than a system with a single nonlinearity that dominates. Thus for mitigation purposes, we must be careful to account for all sources of nonlinearity as suppressing the largest will leave other smaller nonlinearities in the system. Finally, the nonlinearity of the PolM was investigated. We find that when applying a DC bias, the distortion at higher power behaves much differently and cannot be completely mitigated with the HWP. This echoes the conclusion from the partial PDL compensation experiments, that at higher RF power, with multiple nonlinearities in the system, suppression techniques cannot fully mitigate strong distortion.

13

REFERENCES

1. M. N. Hutchinson, N.J. Frigo, and V.J. Urick, "Procedure for aligning polarization modulator link for amplitude modulation applications," Opt. Express, vol. 22, no. 20, pp. 24859 024868, Oct. 2014.

2. X. Chen, W. Li, and J. Yao, "Microwave photonic link with improved dynamic range using a polarization modulator," IEEE Photon. Technol. Lett. 25, 1373-1376 (2013).

3. W. Li and J. Yao, "Dynamic range improvement of a microwave photonic link based on a bi-directional use of a polarization modulator in a Sagnac loop," Opt. Express 21, 15692 (2013).
4. W. Li, L. X. Wang, and N. H. Zhu, "Highly linear microwave photonic link using a polarization modulator in a Sagnac loop," IEEE Photon. Technol. Lett. 26, 89-92(2014).

5. X. Fu, H. Zhang, and M. Yao, "A New proposal of photonic analog-to-digital conversion based on polarization modulator and polarizer," in Proceedings of the 15th Asia-Pacific Conference on Communications (Shanghai, China 2009) pp. 572-574.

6. N. J. Frigo, M. N. Hutchinson and K. E. Thompson, "Polarization-dependent loss in polarization modulated photonic links: Model and Experiment," J. Lightwave Technol., vol. 33, no. 18, pp. 3938-3944, Sept. 2015.

7. M. N. Hutchinson, K. E. Thompson, and N. J. Frigo, "Suppression technique for discrete polarization dependent loss in a polarization modulated link," *in submission*.

8. Jay N. Damask, *Polarization Optics in Telecommunications*. New York, NY, USA: Springer, 2004.

9. N. J. Frigo, "A generalized geometrical representation of coupled mode theory," IEEE. J. Quantum Electron., vol. QE-22, no. 11, pp. 2131–2140, Nov. 1986.

10. J. P. Gordon and H. Kogelnik, "PMD fundamentals: Polarization mode dispersion in optical fibers," Proc. Nat. Acad. Sci., vol. 97, no. 9, pp. 4541–4550, 2000.

11. N. J. Frigo and F. Bucholtz, "Geometrical representation of optical propagation phase," J. Lightw. Technol., vol. 27, no. 15, pp. 3283–3293, Aug. 2009.

12. N. J. Frigo, F. Bucholtz, and C. V. McLaughlin, "Polarization in phase modulated optical links: Jones- and generalized Stokes-space analysis," J. Lightw. Technol., vol. 31, no. 9, pp. 1503–1511, May 2013.

13. C. Vinegoni, M. Karlsson, M. Petersson, and H. Sunnerud, "The statistics of polarization-dependent loss in a recirculating loop," J. Lightw. Technol., vol. 22, no. 4, pp. 968–976, Apr. 2004.

14. J. D. Bull, N. A. F. Jaeger, H. Kato, M. Fairburn, A. Reid, and P. Ghanipour, "40 GHz electro-optic polarization modulator for fiber optic communications systems," Proc. SPIE, vol. 5577, pp. 133–143, 2004.

15. M. N. Hutchinson, N. J. Frigo, and V. J. Urick, "Procedure for aligning polarization modulator link for amplitude modulation applications," Opt. Exp., vol. 22, no. 20, pp. 24859–24868, 2014.

16. M. N. Hutchinson, J. M. Singley, V. J. Urick, S. R. Harmon, J. D. McKinney, and N. J. Frigo, "Mitigation of photodiode induced even-order distortion in photonic links with predistortion modulation," J. Lightw. Technol., vol. 32, no. 20, pp. 3885–3891, Oct. 2014.

17. E. Rudkevich, "Variable polarization dependent loss source," US Patent 6 347 164, Feb. 12, 2002.

18. A. L. Campillo and F. Bucholtz, "Chromatic dispersion effects in analog polarization-modulated links," Applied Optics, vol. 45, no. 12, 2006.

19. J. F. Diehl, J. S. Singley, C. E. Sunderman, and V. J. Urick, "Microwave photonic delay line signal processing," *Appl. Opt.*, vol. 54, no. 31, Nov. 2015.

20. M. N. Hutchinson, S. R. Harmon, V. J. Urick and K. J. Williams, "Analysis of magnitude and relative phase of photodiodes IMD2 using amplitude matched MZM-distortion cancellation technique," *Optics Express*, vol. 22, no. 1, 962-971 (2014).

PDL Inverse Routine

```
dB2lin[dB_] := 10^(dB/10);        (* convert dB to linear units *)

unit[s_] := If[Norm[s] == 0, {0, 0, 1}, s/Norm[s]](* make 3D unit vector *)

(*   power of 'sop' after going thru polarizer oriented at 'pop' where
       p1 is FIELD xmsn thru 'pop' and p2 is FIELD xmsn thru '-pop' *)
pwr[sop_, pop_, p1_, p2_] := (* power *)
  ((p1^2 + p2^2) + (p1^2 - p2^2) (unit[sop].unit[pop])) / 2;

findpdlLIN[polpwrs_] := Module[{sdat, soln, ppop, pdlfit, tran,
    xx, yy, zz, xp, yp, zp, pfx, pfy},
   (* USAGE                                                       *)
   (*  polpwrs is set of {SOP_i, P(lin)}points for 6
     points ...            *)
   (*    { {s11,s12,s13,p1},{s21,s22,s23,p2},                     *)
   (*              ... {s61,s62,s63,p6}  }                        *)
   (*        subroutines needed:  pwr, unit,dB2lin                *)
   (*        FindFit[data, f[pars;vars], pars,  vars]             *)
   soln = FindFit[polpwrs, pwr[{xx, yy, zz}, {xp, yp, zp}, pfx, pfy],
     {xp, yp, zp, pfx, pfy}, {xx, yy, zz}, AccuracyGoal → 4];
   ppop = unit[{xp, yp, zp} /. soln];      (* estimate for pass axis *)
   (* once FIELD xmsns are found, square for intensity *)
   pdlfit = 10 Log10[(pfx / pfy)^2] /. soln;
   (* estimate for PDL magnitude *)
   {pdlfit, ppop} (* return fit *)
  ];

dataSOP = {
   {+.7668, +.5612, -.3115, 57.12},  (* SOP powers in uW *)
   {+.5801, -.8135, -.0257, 41.31},
   {-.5615, +.8235, +.0763, 69.07},
   {-.7488, -.5531, +.3654, 53.52},
   {+.3055, +.1574, +.9394, 68.58},
   {-.2862, -.1773, -.9415, 41.77}
  };

findpdlLIN[dataSOP]

{3.1654, {-0.13498, 0.747118, 0.650842}}
```

APPENDIX B

Lab data fitting 140801 60v2

Functions and constants

```
In[1]:= dBtop = 0;
        dBbot = -140;
        dBlft = -25;
        dBrt = 15;
        pltrng = {{dBlft, dBrt}, {dBbot, dBtop}};
        color = {Blue, Red, Green, Brown};
        npts = 100;
        usin = Table[Sin[2 π n / npts], {n, 0, npts - 1}];
        (* unit sine function for mod input *)

        corr2 = 1.15;  (* THESE ARE COAX LOSS CORRECTIONS FOR 2,4,6,8 GHz *)
        corr4 = 1.62;
        corr6 = 1.92;
        corr8 = 2.46;
```

17

```
a2dB[a_] := 10 Log10[0.5 a^2];          (* convert sine ampl to power *)
dB2a[d_] := Sqrt[2 × 10^(d / 10)];       (* convert power to amplitude *)
spec[power_] := Module[{ft, spectrum},   (* calc 1st 4 Harmonic powers *)
   ft = Fourier[power];
   spectrum = 4 * (.5 Abs[ft]^2) / npts;
   {spectrum[[2]], spectrum[[3]], spectrum[[4]], spectrum[[5]]}
  ];

(*   power of 'sop' after going thru polarizer oriented at 'pop' where
         p1 is FIELD xmsn thru 'pop' and p2 is FIELD xmsn thru '-pop'      *)
pwr[sop_, pop_, p1_, p2_] := ((p1^2 + p2^2) + (p1^2 - p2^2) (unit[sop].unit[pop])) / 2;
unit[s_] := If[Norm[s] == 0, {0, 0, 1}, s / Norm[s]];  (* make 3D unit vector *)
dB2lin[dB_] := 10^(dB / 10);          (* convert dB to linear units *)
lin2dB[lin_] := 10 Log10[lin];  (* convert linear units to dB *)
findpdlLIN[polpwrs_] := Module[{sdat, soln, ppop, pdlfit, tran,
    xx, yy, zz, xp, yp, zp, pfx, pfy},
   (* USAGE                                                      *)
   (* polpwrs is set of {SOPi, P(lin)}points for 6 points ...    *)
   (*   { {s11,s12,s13,p1}, {s21,s22,s23,p2}, ... {s61,s62,s63,p6}  }  *)
   (*          subroutines needed:  pwr, unit, dB2lin            *)
   (*          FindFit[data, f[pars;vars], pars,  vars]          *)
   soln = FindFit[polpwrs, pwr[{xx, yy, zz}, {xp, yp, zp}, pfx, pfy],
     {xp, yp, zp, pfx, pfy}, {xx, yy, zz}];
   ppop = unit[{xp, yp, zp} /. soln];       (* estimate for pass axis *)
   (* once FIELD xmsns are found, square for intensity *)
   pdlfit = 10 Log10[(pfx / pfy)^2] /. soln;   (* estimate for PDL magnitude *)
   {pdlfit, ppop}
  ];
correct[datmat_] := Module[{tr},  (* Apply coax loss corrections to RF data *)
   tr = Transpose[datmat];
   Transpose[{tr[[1]], tr[[2]] + corr2, tr[[3]] + corr4, tr[[4]] + corr6,
     tr[[5]] + corr8}]
  ];

unit[s_] := If[Norm[s] == 0, {0, 0, 1}, s / Norm[s]];  (* makes unit vector *)
flip[r_, s_] := 2 unit[r] (unit[r].s) - s; (* to flip 180, s → spar - sperp *)
flipax[dd_, ss_] := unit[unit[dd] + unit[ss]]; (* parallelogram *)
```

In[25]:=

```
datav0 = {                  (*THIS IS RAW DATA *)
    {-20, -48.12, -123.57, -135.37, -135.16, 2.106, 2.354},
    {-18, -46.08, -119.819, -131.51, -137.43, 2.103, 2.348},
    {-16, -44.09, -115.089, -127.00, -136.34, 2.103, 2.348},
    {-14, -42.12, -111.311, -121.266, -139.74, 2.109, 2.355},
    {-12, -40.15, -107.419, -115.79, -146.62, 2.106, 2.352},
    {-10, -38.14, -104.49, -109.82, -145.81, 2.104, 2.346},
    {-08, -36.12, -98.989, -103.59, -141.21, 2.110, 2.345},
    {-06, -34.13, -94.048, -97.62, -135.76, 2.113, 2.339},
    {-04, -32.14, -89.986, -91.55, -151.93, 2.119, 2.335},
    {-02, -30.19, -85.052, -85.59, -141.1, 2.123, 2.324},
    {+00, -28.18, -79.999, -79.54, -127.38, 2.130, 2.314},
    {+02, -26.29, -74.727, -73.66, -123.78, 2.142, 2.300},
    {+04, -24.39, -69.476, -67.63, -116.337, 2.156, 2.269},
    {+06, -22.50, -63.585, -61.74, -107.711, 2.173, 2.228},
    {+08, -20.77, -57.288, -55.81, -98.059, 2.184, 2.176},
    {+10, -19.15, -51.318, -50.01, -88.410, 2.214, 2.096},
    {+12, -17.84, -45.520, -44.30, -78.295, 2.228, 1.989}};

dataSOP = {
    {-.9795, +.1822, +.0908, 15.58},  (* SOP powers in uW *)
    {+.3015, +.8965, -.3209, 12.83},
    {-.1314, -.9241, +.3600, 13.12},
    {+.9755, -.2174, -.0214, 10.70},
    {+.2080, +.3271, +.9219, 16.60},
    {-.0289, -.3362, -.9412, 9.343}
    };

datav1 = correct[datav0];  (* apply RF coax losses to data *)
```

19

```
In[29]:= sopout = findpdlLIN[dataSOP];
         (*   returns  {extinction in dB, {pass axis P̂}}    *)
         tp = 10^(-sopout[[1]] / 20);   (* transmission for PDL *)
         PPhat0 = sopout[[2]];  (* P̂ for PDL *)
         PP0 = PPhat0 (1 - tp) / 2;  (* P̂ for PDL *)
         p0 = (1 + tp) / 2;
         pbar = (1 - tp) / 2;
         SS = {.9686, -.2384, .0610};  (* from experiment after 90 deg rotation *)
         DD = {0, 0, 1};
         DDhat = unit[DD];  (*image of detector axis on PA *)
         MM = DDhat × SS;  (* image of modulator eigenstate *)
         rr = flipax[DD, SS];  (* find HWP flipping axis as bisector of DD⃗ and SS⃗ *)
         PP = flip[rr, PP0];  (* flip the P̂ vector image on the PA *)
         PPhat = unit[PP];
         PHI = ArcCos[PPhat.unit[DD]];
         AA = ((Cos[PHI / 2])^2 + tp (Sin[PHI / 2])^2) PP + tp DDhat / 2;
         CC2 = -(MM × AA.SS + (AA.MM) (MM.SS));
         CC3 = AA.SS;

In[46]:= s3 = Sqrt[3];
         thk = 0.2;
         circle = Graphics[{Thickness[thk], Circle[{0, 0}]}];
         plus =
           Graphics[{Thickness[thk], Line[{{-.5, 0}, {0.5, 0}, {0, 0}, {0, .5}, {0, -.5}}]}];
         triangle =
           Graphics[
             {Thickness[thk], Line[{{-.5, -s3 / 6}, {.5, -s3 / 6}, {0, s3 / 3}, {-.5, -s3 / 6}}]}];
         square =
           Graphics[
             {Thickness[thk], Line[{{-.5, -.5}, {.5, -.5}, {.5, .5}, {-.5, .5}, {-.5, -.5}}]}];
         tr = Transpose[datav1];  (* create plots of data points to help fit model *)
         fundraw = Transpose[{tr[[1]], tr[[2]]}];
         secondraw = Transpose[{tr[[1]], tr[[3]]}];
         secondtrim = secondraw[[3 ;; Length[secondraw]]];
         thirdraw = Transpose[{tr[[1]], tr[[4]]}];
         thirdtrim = thirdraw[[3 ;; Length[thirdraw]]];
         fourthraw = Transpose[{tr[[1]], tr[[5]]}];
         fourthtrim = fourthraw[[10 ;; Length[fourthraw]]];
         fund = ListPlot[fundraw, PlotMarkers → {circle, .05}, PlotRange → pltrng,
             Frame → True, Axes → False ];
         third = ListPlot[thirdtrim, PlotMarkers → {triangle, .05}];
         second = ListPlot[secondraw, PlotMarkers → {plus, 0.05}];
         second = ListPlot[secondtrim, PlotMarkers → {plus, 0.05}];
         fourth = ListPlot[fourthtrim, PlotMarkers → {square, .05}];

In[65]:= Transpose[{tr[[1]], tr[[2]]}];

In[66]:= Manipulate[
```

```
ppts =
  Show @@
    (ListPlot[Transpose[pptsout][[#]], PlotStyle → {color[[#]], PointSize[.008]},
        PlotRange → pltrng, Frame → True, Axes → False ] & /@ {1, 2, 3, 4});

label = Graphics[{Text[Style["PDL 60", 24, FontFamily → "Helvetica"], {-20, -20}]}];
Show[(*g3ext,g2ext,g4ext,*)fund, second, third, fourth, ppts, label,
  FrameLabel → {"PolM input dBm", "ESA output dBm"},
  LabelStyle → Directive[Large, FontFamily → "Helvetica"]],
{{a2, -.022}, -.4, .4}, {{Φb, 0.378}, -.6, .6}, {{eps, 0.014}, -.4, .4},
{{RFIN, 14.6}, 10, 20}, {{RFOUT, 2
 }, 0, 25}, SaveDefinitions → True
]
```

Out[66]=

21